Dynamic Transitions of the Transmembrane Domain of Diphtheria Toxin: Disulfide Trapping and Fluorescence Proximity Studies†

Hangjun Zhan,‡ Senyon Choe,§,‖ Paul D. Huynh,⊥ Alan Finkelstein,⊥ David Eisenberg,§ and R. John Collier*,‡

Department of Microbiology and Molecular Genetics and Shipley Institute of Medicine, Harvard Medical School, 200 Longwood Avenue, Boston, Massachusetts 02115, Department of Physiology & Biophysics and Neuroscience, Albert Einstein College of Medicine, 1300 Morris Park Avenue, Bronx, New York 10461, and Molecular Biology Institute, Department of Chemsitry and Biochemistry, and UCLA-DOE Laboratory of Structural Biology and Molecular Medicine, University of California, Los Angeles, California 90024-1570

Received June 2, 1994; Revised Manuscript Received July 19, 1994®

ABSTRACT: Translocation of the catalytic domain of diphtheria toxin across the endosomal membrane to the cytosolic compartment depends on low-pH-triggered insertion of the toxin's T (transmembrane) domain into the membrane. The T domain, consisting of nine α-helices arranged in three layers, was cloned and expressed as a discrete protein in *Escherichia coli,* and mutant forms were prepared and characterized. To investigate the relative movements of the three layers under various conditions, we generated two mutant forms of the domain, each containing an artificial intramolecular disulfide bridge linking the buried apolar hairpin (TH8–TH9) to one of the other two layers. Both disulfides inhibited exposure of the domain's apolar regions in solution at low pH, as determined by 2-*p*-toluidinylnaphthalene-6-sulfonate binding, and blocked its ability to form channels in artificial bilayers. Reduction of the bridges abolished these effects. Reduced forms of the mutant proteins were reacted with pyrenylmaleimide, a fluorescent probe, to monitor separation of the layers. Strong excimer bands seen in both mutants at neutral pH were undiminished at pH 5, indicating the retention of gross conformation in solution under acidic conditions. The addition of phospholipid vesicles at pH 5, but not at pH 7.5, quenched excimer fluorescence, reflecting the physical separation of the TH8–TH9 hairpin from the other layers upon the T domain's interaction with the bilayer. The results indicate that (i) the conformation of the isolated T domain closely resembles that seen in the whole toxin, (ii) the TH8–TH9 hairpin separates from both of the other layers of the domain as an essential step of membrane insertion, and (iii) this separation is triggered by contact of the domain with the membrane under acidic conditions.

Diphtheria toxin (DT[1]) has become an important model for understanding the mechanisms by which toxic proteins damage human cells (Collier, 1990; London, 1992). In recent years, many of the most potent toxic proteins, including DT, have been found to be sophisticated enzymes, which have the ability to convey their enzymic moieties across a membrane barrier into the cytoplasmic compartment of sensitive cells. The process of membrane traversal by macromolecules is of fundamental importance in biology and is not fully understood for any protein, including toxins. Now that the crystallographic structure of DT is known (Choe *et al.,* 1992), one has a firm basis for pursuing its various functions, including membrane traversal, at the atomic level.

Diphtheria toxin is secreted by *Corynebacterium diphtheriae* as a 58 kDa polypeptide that is readily cleaved proteolytically into an N-terminal 21 kDa fragment (fragment A) and a C-terminal 37 kDa fragment (fragment B) joined by a disulfide bond. The B fragment is responsible for binding to receptors and mediating translocation of the A fragment into the cytoplasm of sensitive cells. There, the A fragment inhibits protein synthesis by catalyzing the ADP-ribosylation of elongation factor-2, which results in cell death.

After binding to its receptor, a heparin-binding EGF-like growth factor precursor (Naglich *et al.,* 1992), DT undergoes receptor-mediated endocytosis and is transported to the endosomal compartment. Exposure to the acidic lumen of the endosome triggers the toxin to insert into the endosomal membrane, which leads to translocation of the catalytic domain (fragment A) across the membrane (Sandvig & Olsnes, 1980, 1981; Draper & Simon, 1980). Besides being a key step in translocation, the insertion represents an interesting example of the transformation of a protein from a soluble, globular form to an integral membrane form. Acidic endosomal pH has also been shown to trigger the translocation of several other toxins and many mammalian viruses (Davis *et al.,* 1990).

The crystal structure of DT, determined at 2.5 Å resolution (Choe *et al.,* 1992), reveals a Y-shaped molecule of three discrete domains: the catalytic domain (C, amino terminus), the transmembrane domain (T, intermediate), and the receptor binding domain (R, carboxyl terminus). Fragment A corresponds to the C domain, and fragment B contains both the T and R domains. The T domain, which is known to undergo pH-triggered insertion into membranes, consists of nine α-helices arranged in three layers. The innermost layer is composed of a long buried helical hairpin, containing two apolar helices (TH8, 21 residues, and TH9, 23 residues) connected by an acidic loop (TL5). The intermediate layer

† This work was supported by NIH Grants AI22021 and AI22848 (to R.J.C.), GM29210 (to A.F.), and T32GM07288 (to P.D.H.).

* Author to whom correspondence should be addressed.
‡ Harvard Medical School.
§ University of California at Los Angeles.
‖ Present address: The Salk Institute, La Jolla, CA 92037.
⊥ Albert Einstein College of Medicine.

® Abstract published in *Advance ACS Abstracts,* September 1, 1994.

[1] Abbreviations: DOPG, 1,2-dioleoyl-*sn*-glycero-3-phosphatidylglycerol; DT, diphtheria toxin; DTT, dithiothreitol; EDTA, ethylenediaminetetraacetic acid; TNS, 2-*p*-toluidinylnaphthalene-6-sulfonate; PC, phosphatidylcholine; PM, *N*-(1-pyrenyl)maleimide; SDS–PAGE, sodium dodecyl sulfate–polyacrylamide gel electrophoresis; Tris, tris(hydroxymethyl)aminomethane.

0006-2960/94/0433-11254$04.50/0

consists of helices TH5, TH6, and TH7 and the TL3 loop (between TH5 and TH6), which together form another apolar, kinked hairpin wrapping around the innermost layer. The outermost layer, consisting of helices TH1–TH4 (and including the TL2 loop), contains a high density of charged residues and is considered unlikely to insert into membranes.

Choe *et al.* (1992) proposed, on the basis of the crystal structure, that the apolar helical hairpin formed by TH8 and TH9, and possibly the TH5–TH7 hairpin as well, might represent a membrane-soluble motif that would insert into a membrane bilayer after partial unfolding of the T domain at acidic pH. The acidic residues within the TL3 and TL5 loops would become at least partially protonated under acidic conditions within the endosome, rendering them more membrane-soluble. According to this model, these residues should reionize upon exposure to neutral conditions after the acidic loop(s) penetrates to the cytosolic face of the membrane, thereby locking the hairpin(s) in the membrane. Helices TH1–TH3 should be positively charged at pH 5.0 and might be expected to spread on the surface of the bilayer and interact electrostatically with negatively charged phosphate head groups of phospholipids.

Recent findings have lent support to certain aspects of this model. Substitution of a lysine within the TL5 loop, to replace either Glu349 (O'Keefe *et al.*, 1992) or Asp352 (Silverman *et al.*, submitted for publication), greatly reduced toxicity and channel formation. This result is consistent with the notion that the TH8–TH9 hairpin normally undergoes membrane insertion and that this insertion is necessary for translocation. Other recent studies have shown that the TH8–TH9 hairpin alone is sufficient for the formation of channels in membranes, although it is inefficient without the remainder of the T domain (Silverman *et al.*, 1994). Furthermore, at least some residues within the loop region of the TH8–TH9 hairpin are accessible to the trans side after membrane insertion in the planar bilayer (Mindell *et al.*, 1994a,b). On the other hand, current data give no clear indication whether the other hairpin, TH5–TH7, inserts into the membrane (Silverman *et al.*, 1994). Thus, accumulated evidence points to the TH8–TH9 hairpin as the major structural element of the T domain that becomes embedded in the bilayer and anchors the toxin to the membrane.

Membrane insertion of the apolar TH8–TH9 hairpin at low pH, and the consequent conversion of the T domain to an integral membrane form, would clearly require the domain to undergo major conformational changes. To investigate and evaluate such structural rearrangements, we have studied the proximity relationships of selected sites within the T domain under a variety of conditions. Specifically, we introduced pairs of Cys residues into the Cys-free T domain and used their SH-containing side chains (i) to generate disulfide bridges that restrict the relative motions of the three layers and (ii) to serve as attachment sites of fluorophoric probes useful in sensing the proximity of the layers. The results reveal insights into the conformational changes required for membrane insertion and the respective roles of pH and membrane contact in inducing these changes.

EXPERIMENTAL PROCEDURES

Site-Directed Mutagenesis. Mutagenic oligonucleotides were synthesized and purified as described (Hovde *et al.*, 1988). Site-directed mutagenesis was performed using the mutagenesis system, version 2.1, from Amersham, according to the manufacturer's instructions. The phage M13mp18::DT vector containing the entire diphtheria toxin gene sequence (with the E148S substitution to ablate enzyme activity) was constructed by inserting the *Bam*HI–*Eco*RI fragment from pDOl (O'Keefe & Collier, 1992) into M13mp18, and the single-stranded form was used as a template for the mutagenesis. Mutations were verified by DNA sequencing with Sequenase (United States Biochemicals). Other DNA manipulations were performed basically as described by Ausubel *et al.* (1987). All of the restriction enzymes and T4 DNA ligase were purchased from New England Biolabs.

T-Domain Expression and Purification. Mutant forms of the T domain were cloned into pET-15b-T, a derivative of pET-15b (Novagen), for overexpression and purification. The expressed protein contained residues 202–378, plus four vector-encoded residues at their N-terminus: Gly-Ser-His-Met. The single cysteine in the native T domain, Cys201, was therefore excluded from this construct, giving a Cys-free background for analysis. The numbering of the T domain corresponds to that in native DT (Greenfield *et al.*, 1983). Details of the construction of pET-15b-T will be published elsewhere (Zhan *et al.*, manuscript in preparation). Expression was under the control of the strong bacteriophage T7 transcription and translation signals. The expression and purification procedures were the same as those described for the pET by Novagen, except that the washing volume was 30 times the column bed volume. All four mutants were expressed in *Escherichia coli* BL21(DE3) (Studier & Moffatt, 1986). Cultures were induced by addition of isopropyl β-D-thiogalactopyranoside to a final concentration of 1 mM, and after a 2 h induction at 37 °C, cells were harvarsted and sonicated on ice. The Cys mutant T domains were purified using Ni^{2+}-charged His-binding columns eluted with 1 M imidazole. The eluents were dialyzed for 16 h against three changes of argon-flushed 20 mM Tris-HCl (pH 8.0), containing 2 mM DTT. The protein samples were concentrated using Centriprep 10 and Centricon 10 (Amicon) filters. The N-terminal hexahistidine tag was removed with thrombin, and further purification was achieved by anion exchange column chromatography (Pharmacia, Mono Q). All of the proteins were stored at −70 °C in Tris-HCl buffer (20 mM, pH 8.0) and 2 mM DTT.

The identity of all the mutant T domains was confirmed by Western immunoblotting, with anti-DT antiserum (Cannaught) as the primary antibody and goat anti-rabbit alkaline phosphatase conjugate as the secondary antibody. Blots were developed with 5-bromo-4-chloro-3-indolyl phosphate as the chromagenic substrate. The presence of the engineered cysteine(s) in each mutant protein was verified by removing DTT and labeling with fluorescein maleimide, followed by SDS–polyacrylamide gel electrophoresis. The fluorescence of protein bands in the gel was visualized with an ultraviolet transilluminator, and the gel was subsquently stained with Coomassie to confirm the protein bands. Protein concentrations were determined by using Coomassie reagent (Pierce) with BSA as the standard.

Disufide Bond Formation and Quantification. T domains containing single or double Cys mutations were diluted to 0.5 μM in reaction buffer (20 mM sodium phosphate, 100 mM NaCl, and 1 mM $NaAsO_2$, pH 7.2). The protocol of oxidative disulfide formation reaction was essentially as described (Careaga & Falke, 1992). Disulfide formation was catalyzed by copper(II) (1,10-phenanthroline)$_3$ with ambient dissolved oxygen as the oxidant (Kobashi, 1968). After incubation, the reaction mixture was dialyzed against three changes of 20 mM Tris-HCl (pH 8.0), and the proteins were concentrated to 1 mg/mL using Centriprep 10 filters. The disulfide-containing and disulfide-free products were resolved on 13%

SDS–polyacrylamide gels run in the presence or absence of DTT. T domains containing an intramolecular disulfide migrated faster on SDS–polyacrylamide gel than those lacking a disulfide, which comigrated with the wild-type T domain. Addition of DTT to the disulfide-containing forms restored wild-type mobility. Gels from nonreducing SDS–PAGE were stained with Coomassie Blue R-250, and the percentage of intramolecular disulfide bonds formed was quantified with an UltroScan XL laser scanning densitometer.

Channel Measurements. Planar lipid bilayer membranes were formed at room temperature, using a modification of the folded film method of Montal (1974), across a hole (90–100 μm diameter) in a polystyrene cup (Wonderlin *et al.*, 1990). To form a membrane, the hole was precoated on each side with 5 μL of a 1% hexane solution of asolectin [lecithin type IIS (Sigma Chemical Co., St. Louis, MO) from which neutral lipids had been removed by the method of Kagawa and Racker (1971)], allowed to dry, and then precoated on the outside of the cup with 5 μL of squalene (1% in petroleum ether). Fifty microliters of the same asolectin solution was layered on buffered salt solution outside the cup above the level of the hole, and the hexane was allowed to evaporate. The solution was then lowered and raised to form a bilayer. The volumes outside and inside the cup were 1 and 0.5 mL, respectively. Bridges containing 3 M KCl in 3% agar connected the solutions inside and outside the cup to Ag/AgCl electrodes in 3 M KCl baths. Membrane formation was monitored through measurements of the system capacitance, using the voltage clamp with a triangle wave input; membrane conductances were less than 1 pS. Both solutions contained 1 M KCl, 2 mM $CaCl_2$, and 1 mM EDTA; the exterior solution also contained 30 mM MES, pH 5.3, and that within the cup contained 50 mM HEPES, pH 7.2. After the membrane was formed, T-domain S291C/V351C or N235C/V351C (oxidized or reduced) was added to the outside solution (defined as the cis side), which was stirred with a miniature magnetic stir-bar, to a final concentration of tens of nanograms/milliliter, and known voltages were applied across the membrane. Voltages were those of the cis compartment; the potential of the trans compartment was taken as zero. Membranes were voltage clamped using an EPC-7 patch-clamp amplifier (List Medical Systems, Darmstadt, Germany), and current was monitored on a chart recorder.

Stock solutions of oxidized T-domain C291/C351[2] and C235/C351 in 20 mM Tris-HCl, pH 8.0, were stored at −70 °C. For a given day's experiment, a small aliquot was taken and diluted to 10 μg/mL. This diluted sample was divided in half, and to one portion was added DTT to a concentration of 20 mM and kept for 10 min at room temperature in order to reduce the internal disulfide bond; the reduced and unreduced portions were then kept on ice for the remainder of the day. To compare the channel-forming activity of the unreduced and reduced forms of the protein, a given amount of unreduced protein was added to the cis compartment, and then after several minutes a smaller amount of reduced protein was added to the same compartment. Throughout this time, the membrane current in response to an applied voltage of +60 mV was continually monitored.

TNS-Dependent Sensing of Protein Unfolding. The detailed protocol was as described previously (Koehler & Collier, 1991). T domain (175 nM) was incubated with 150 μM TNS (Molecular Probes) for 20 min at room temperature in 100 mM buffer (Tris-HCl for pH 8.0 and 7.0; MES for pH 6.5 and 6.0; sodium acetate for pH 5.5, 5.0, 4.75, and 4.5) containing 150 mM NaCl and 1 mM EDTA. The florescence emission spectrum of the sample was recorded at 25 °C (excitation wavelength, 366 nm; bandpass, 5.0; and emission wavelength 440 nm) in an SPF-500C spectrofluorometer (Aminco).

Liposome (Small Unilamellar Vesicle) Preparation. Twenty milligrams of a lipid mixture composed of DOPG (20% w/w) and PC (80% w/w) (Avanti Polar Lipids) in chloroform was dried uniformly onto the sides of a 25 mL pear-shaped flask under a stream of nitrogen and then dried further under high vacuum for 3 h. The dried lipid film was hydrated in 2 mL of buffer containing 10 mM Tris-HCl, pH 7.5, 0.1 mM EDTA, and 140 mM NaCl. The suspension was then sonicated on ice in a Branson Model 350 sonifier until nearly optically clear. Care was taken to avoid heating the lipid suspension during sonication.

Proximity Studies by Cys-Specific Fluorescence Labeling. Cys residues were labeled with *N*-(1-pyrenyl)maleimide (PM) (Molecular Probes) as follows: Proteins stored with 2 mM DTT were dialyzed against two changes of argon-flushed 20 mM Tris-HCl, pH 7.5, for 2 h. PM dissolved in *N*,*N*-dimethylformamide (DMF) at a concentration of 6 mM was slowly added to the dialyzed sample until a 30-fold molar excess of the reagent to protein was achieved. The final volume ratio of the organic solvent (DMF) to the sample solution was less than 1%. The reaction mixture was incubated at room temperature for 3 h in the dark. After incubation, the reaction mixture was centrifuged at 16000*g* for 5 min to remove undissolved reagent. The supernatant was then dialyzed overnight in the dark at 4 °C in 20 mM Tris-HCl, pH 8.0, with three changes. The amount of PM covalently bound was estimated by measuring the absorption of pyrene and determining the concentration, assuming an extinction coefficient of $2.2 \times 10^4\ M^{-1}\ cm^{-1}$ at 340 nm (Kouyama & Mihashi, 1981). The double mutants contained ~0.8 mol of PM/mol of protein and the single mutants ~0.6.

Fluorescence emission spectra were recorded with constant stirring at 25 °C using an Aminco SLM 500 spectrofluorometer. The temperature was controlled by a circulating water bath. The excitation wavelength was 344 nm.

RESULTS

Design, Construction, and Expression of Mutant T Domains. A focal point for the study of conformational changes of the T domain is presented by a region in which loops of the three α-helical layers are in close proximity (Figure 1). Within the native toxin, the TL5 loop, at the tip of the buried helical TH8–TH9 hairpin, is close to both the TL2 loop of the TH1–TH4 layer and the tip of the TH5–TH7 hairpin [in the original model, the tip was described simply as a loop (TL3), but in the refined model this region was found to contain a short helix, designated TH5′ (Bennett *et al.*, 1994)]. This offers the possibility of linking the TH8–TH9 hairpin to each of the other layers by artificial disulfides as a means of inhibiting pH-mediated unfolding. Also, probes such as fluorophores can be introduced by covalent reaction with the sulfhydryl groups to study the proximity relationships of the layers under various conditions. We therefore searched, using the algorithm of Proteus (Pabo & Suchanek, 1986), for pairs of residues within these loops that would be suitable locations for Cys replacements for the purposes indicated. Uncharged and solvent-exposed residues were chosen to minimize the possible disruption of function and to maximize the accessibility and

[2] C235, C291, and C351 are used instead of N235C, S291C, and V351C, respectively, at positions in the text where the former designations seem more logical.

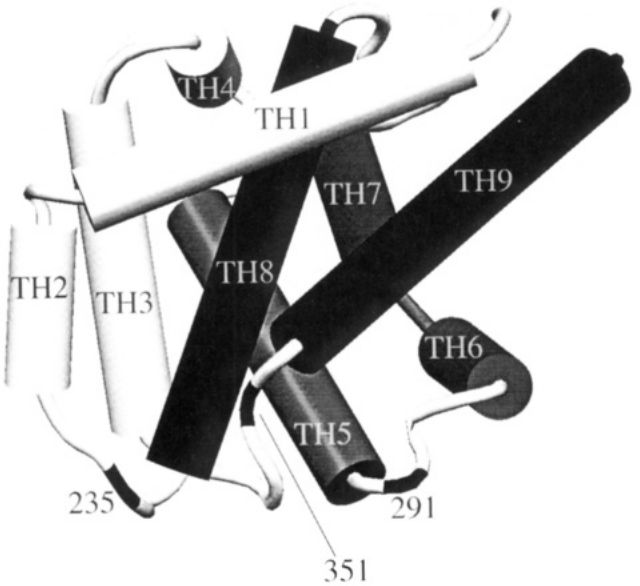

FIGURE 1: Schematic representation of the tertiary structure of the T domain based on the crystal structure originally described by Choe *et al.* (1992), as refined by Bennett *et al.* (submitted for publication). Helices 1–9 are shown, organized as three layers: outermost layer (TH1–TH4), light shading; intermediate layer (TH5–TH7), intermediate shading; innermost layer (TH8–TH9), black. The residues selected for replacement by Cys (N235, S291, and V351) are indicated.

reactivity of the sulfhydryl groups introduced. The pairs, S291/V351, with 8 Å between the two α-carbons, and N235/V351, with 13.3 Å between the α-carbons, were selected. A disulfide link between C235, within TL2, and C351, within TH5′, would be expected to prevent separation of the highly charged outer layer from the innermost layer, TH8–TH9, and a disulfide between C291 and C351 would covalently connect TL3 and TL5, thereby restricting the movement of the intermediate, TH5–TH7, layer with respect to TH8–TH9 (Figures 1 and 2). The flexibility of the regions in which the Cys residues were introduced, as judged by X-ray thermal factors, might be expected to facilitate disulfide formation.

The Cys replacements were generated in a cloned form of the T domain (residues 202–378), with an N-terminus selected so as to eliminate the sole native Cys in this region, Cys201, residing within the loop connecting the T and C domains. Also, a hexahistidine affinity tag was appended to the amino terminus to permit purification by nickel chelate affinity chromatography. The single mutations (N235C, S291C, and V351C) were generated first, and the double Cys mutants (N235C/V351C and S291C/V351C) were then prepared from the V351C mutant template. All of the single and double Cys mutants were expressed cytoplasmically in *E. coli*, and the T domain was purified from the soluble fraction of cell sonicates. Inclusion bodies, which constituted ca. 30% of the T-domain protein, were excluded, and no denaturants were used during the process of purification. After affinity purification of the protein, the N-terminal hexahistidine tag was removed by thrombin digestion, and the protein was purified further by anion exchange chromatography. The product was >95% pure, based on laser densitometry of SDS–polyacrylamide gels, had the expected molecular weight, and was reactive with anti-DT polyclonal antiserum on Western blots. Evidence to be presented elsewhere indicates that the T domain is monomeric in solution at neutral pH and at pH 5 (Zhan *et al.*, manuscript in preparation). When stored in the presence of 2 mM DTT, the wild-type and mutant proteins were stable for weeks at 4 °C. All of the Cys mutants gave yields comparable to that of the wild-type T domain (~2.5 mg/L of culture).

Intramolecular Disulfide Formation. Proteins with internal disulfides usually have higher mobilities on SDS–polyacrylamide gels than their reduced counterparts, enabling one to assess intramolecular disulfide formation by comparing electrophoretic mobilities in the presence and absence of reducing agents. After the removal of DTT, intramolecular disulfide bond formation was negligible in either the C235/C351 or the C291/C351 protein by this criterion, for a 24 h incubation at room temperature. However, noticeable intermolecular disulfide formation was seen with both the double Cys and the single Cys mutants (at protein concentrations ≥0.5 mg/mL), as evidenced by the appearance of T-domain dimers on nonreducing gels. No dimer was observed with a control T domain lacking Cys. The observation that intermolecular disulfide bonds formed readily between all three single mutant proteins is consistent with their solvent exposure, as expected from the crystal structure, if the isolated T domain maintains the conformation observed in whole DT.

To accelerate intramolecular disulfide formation in the double Cys mutants, copper(II) (1,10-phenanthroline)$_3$ was used as a catalyst to promote oxidation by ambient oxygen. Relatively low concentrations of protein (≤0.5 μM) were employed to avoid intermolecular disulfide formation. Under these conditions, the C291/C351 T domain was rapidly and quantitatively converted to the more rapidly migrating, intramolecular disufide-containing form (Figure 3); the reaction was complete within 40 min. With the C235/C351 mutant, however, only ~75% of the protein was converted to the intramolecular disulfide-containing form, as judged by scanning densitometry of SDS–polyacrylamide gels. The lower efficiency of internal disulfide formation for the C235/C351 mutant may reflect the difficulty of closing the greater distance between the two residues or their suboptimal orientations relative to one another.

We attempted, by various means, to obtain pure disulfide-containing C235/C351 mutant, but without success. Variations in the pH, salt, reaction time, or combinations thereof failed to improve the efficiency of internal disufide formation. We were unable to resolve the disulfide-containing and disulfide-free forms by anion exchange chromatography, and attempts to remove the disulfide-free form selectively on an SH-specific organomercury affinity gel (Affi-gel 501, Bio-Rad) failed due to the high affinity of the wild-type T domain for the resin. Lastly, attempts to react any free sulfhydryl groups in the protein with reactive biotin failed. These observations are consistent with the O_2/copper(II) (1,10-phenanthroline)$_3$ redox chemistry, which yields both disulfide bonds and either the sulfinic (SO_2^-) or the sulfonic (SO_3^-) oxyacid as the unproductive sulfhydryl oxidation product. After the 40 min reaction, the sulfhydryl groups that had not entered into disulfide linkages apparently had been oxidized to unproductive products. No further efforts were made to separate the various forms, and measurements made on the C235/C351 mutant were performed on the mixture of disulfide-containing and disulfide-free forms (ratio ~3:1).

Channel Formation. At acidic pH, DT or isolated T domain is capable of inserting into artificial lipid bilayers and forming voltage-gated ion channels (Kagan *et al.*, 1981; Mindell *et al.*, 1994b). Channel formation reflects the ability of the protein to insert into the membrane, and single-channel conductance measurements may be used to probe the structure of the DT channel. Current records were analyzed both for channel-forming activity (assessed by the number of channels

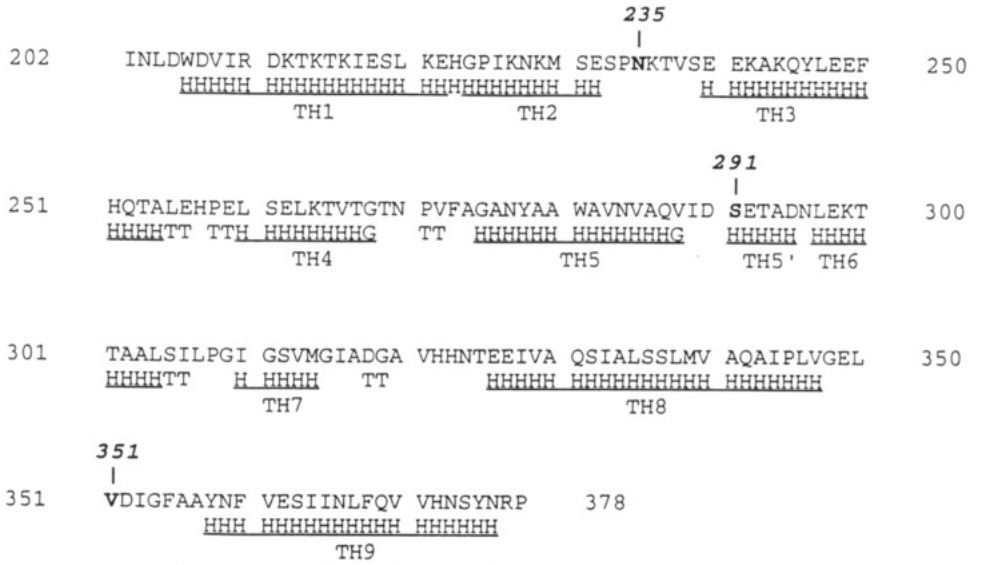

FIGURE 2: Secondary structure assignments of T domain [adapted from Figure 8 of Bennett *et al.* (submitted for publication)]. Upper line represents the amino acid sequence (Greenfield *et al.*, 1983); second line indicates the visual secondary structure assignment, using the nomenclature of Kabsch and Sander (1983): G, 3_{10}-helix; H, α-helix; T, hydrogen-bonded turn. The TL3 loop in the original model of Choe *et al.* (1992) (residues 289–296) was shown in the refined model of Bennett *et al.* (submitted for publication) to contain a short helix, labeled TH5′, as indicated. Loop TL5 corresponds to residues linking TH8 and TH9.

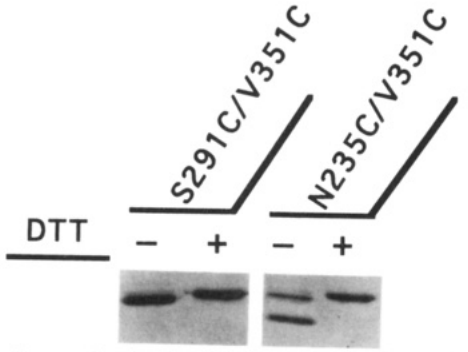

FIGURE 3: Intramolecular disulfide formation, as detected on SDS–polyacrylamide gels in the presence or absence of reducing agent. The oxidized T domains of S291C/V351C and N235C/V351C were mixed with SDS loading buffer in the presence or absence of 20 mM DTT. The mixtures were boiled for 3 min, and 2 μg of sample was loaded on each lane of 13% SDS–PAGE. The gel was then stained with Coomassie. Note that the oxidized (trapped) forms for both double mutants showed higher mobilities.

produced by a given amount of protein within a given period) and for the current carried by individual channels (single-channel conductance). The reduced forms containing each of the Cys replacements—including C235, C291, C351, C235/C351, and C291/C351—showed the same activity as wild-type T domain in forming conductive channels in asolectin bilayers under conditions that mimic those of the endosome (pH 5.3 on the cis side, or the T domain-containing chamber, and pH 7.2 on the trans side). Single-channel conductance of channels formed by C235/C351 and C291/C351 T domains was similar to that of channels formed by wide-type T domain or DT. These results indicate that the Cys replacements *per se* did not alter the channel-forming properties of the T domain or the structure of the channel formed.

The channel-forming abilities of the oxidized forms of both the C291/C351 and C235/C351 T domains were found to be greatly diminished relative to those of their corresponding reduced forms. Figure 4 shows an example of this for the C291/C351 mutant. Seven minutes after exposure to 30 ng/mL of its oxidized form, the membrane conductance had increased to only 730 pS, whereas 3 min after subsequent exposure to 10 ng/mL of its reduced form, the conductance had reached 9000 pS and was still increasing linearly. Thus, the reduced form of the C291/C351 mutant was at least 100-fold more active than its oxidized form. The residual activity of the oxidized form may have been caused by undetected, untrapped species. Similar experiments with the C235/C351 mutant showed that its reduced form was at least 25-fold more active than its oxidized form.[3] These results, as a whole, indicate that covalent bonding of the TL5 loop to either TL2 or TL3 strongly inhibited the protein's channel-forming capability.

pH-Dependent TNS Binding. The profile of binding of hydrophobic fluorophores by DT or the T domain as a function of pH is a useful reference in studying conformational alterations attendant to insertion. The effects of the C291/C351 and C235/C351 disulfides on pH-dependent conformational alterations of the T domain were investigated with the TNS binding assay. The fluorophore TNS (2-*p*-toluidinylnaphthalene-6-sulfonate), which exhibits a much higher quantum yield in apolar environments than in aqueous ones, has been employed as a probe of apolar sites on the protein (Collins & Collier, 1987). Reduced and oxidized forms of the mutants were dialyzed against argon-flushed 10 mM Tris-HCl buffer, pH 8.0, for 2 h with two changes of buffer to remove DTT, a strong quencher of TNS fluorescence, from the reduced samples. Each of the samples (175 nM) was then incubated with 150 μM TNS for 20 min at room temperature in 100 mM buffer containing 150 mM NaCl and 1 mM EDTA at pH 8.0, 7.0, 6.5, 5.5, 5.25, 5.0, 4.75, and 4.5. As illustrated in Figure 5A, TNS fluorescence showed a dramatic increase between pH 5.5 and 5.0 with the wild-type T domain, reflecting the exposure of cryptic apolar surfaces. Similar pH dependence profiles were observed with 5, 50, or 150 μM TNS. With C291/C351, the oxidized form gave a greatly diminished change in the pH-dependent fluorescence relative to the reduced form, which showed a profile similar to that of the wild-type protein. Thus, the disulfide bond between C291

[3] The oxidized form of the C235/C351 mutant showed very low channel-forming activity, despite the fact that ca. 25% of it apparently was not in the disulfide-trapped state. This may be attributable to the inhibition of membrane insertion of the TH8–TH9 hairpin by negatively charged oxidation products, SO_2^- and/or SO_3^-, at position 351.

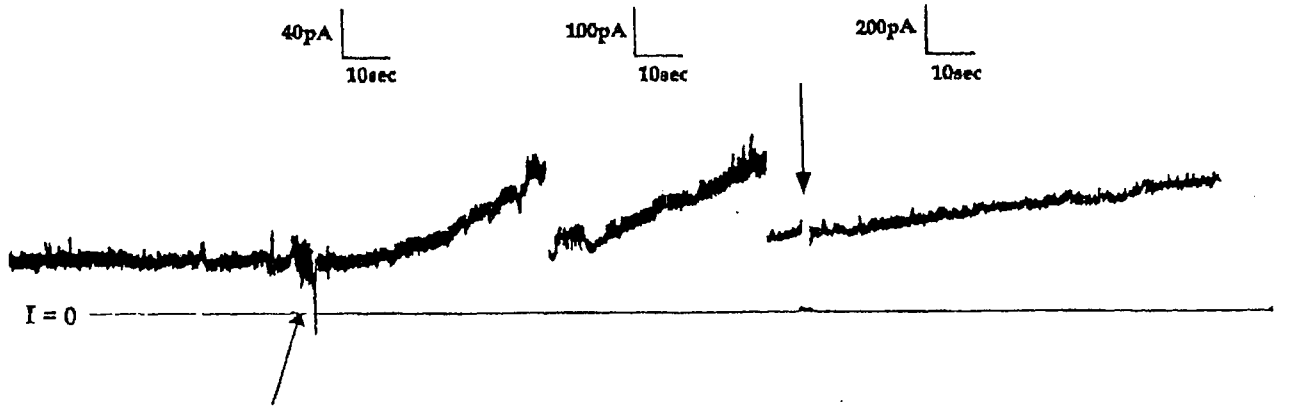

FIGURE 4: Comparison of the relative channel-forming activity in a planar lipid bilayer of the oxidized and reduced forms of T domain C291/C351. Before the start of the recording, 30 ng of oxidized C291/C351 was added to the cis compartment, which was stirred continuously throughout the experiment. Channels were inserted slowly into the membrane; after 7 min, when the recording begins, the conductance had reached only 730 pS (about 18 open channels). At the arrow, an additional 10 ng of reduced C291/C351 was added to the same compartment. Note the rapid increase in conductance produced by the reduced form of the protein. During the entire recording, the potential across the membrane was held at +60 mV (except for 2 s at 0 mV, seen in the last segment of the recording, second arrow).

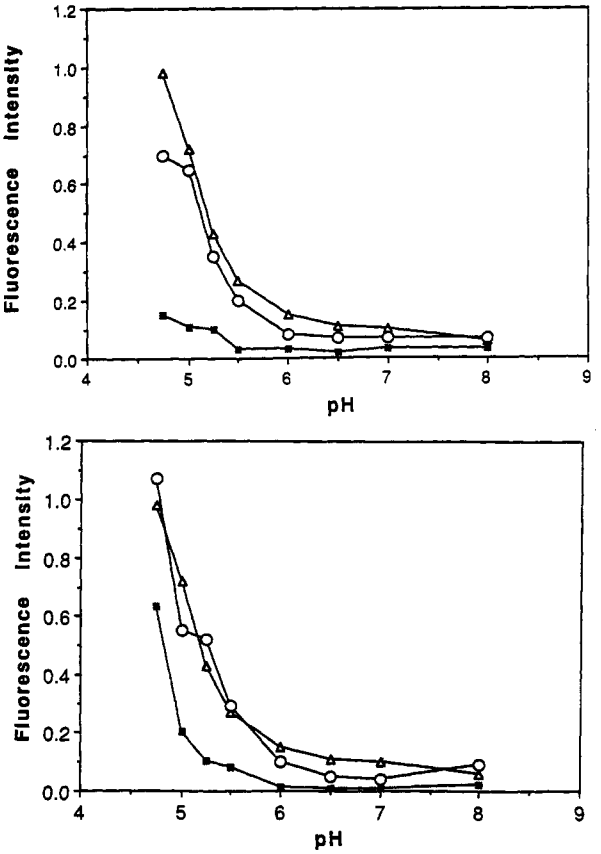

FIGURE 5: Effect of intramolecular disulfide bonds on pH-dependent conformational changes, as determined by TNS fluorescence. Proteins were diluted to 175 nM in 150 μM TNS at the pH indicated and incubated for 20 min at room temperature. The fluorescence was determined at 25 °C. The excitation wavelength was 366 nm, and the emission wavelength was 440 nm. (A, top) Double mutant S291C/V351C in oxidized (■) and reduced forms (○), with the wild-type T domain as a reference (△). (B, bottom) Double mutant N235C/V351C in oxidized (■) and reduced forms (○), with the wild-type T domain as control (△).

and C351 blocked exposure of the embedded apolar sites at acidic pH. Qualitatively similar results were seen with the C235/C351 T domain (Figure 5B), but the fluorescence increase observed at low pH with the oxidized form was greater than that with the C291/C351 mutant, probably due to the greater levels of the disulfide-free form present. The fact that the pH-dependent fluorescence profiles of the reduced forms of both C235/C351 and C291/C351 mutants were similar to that of the wild type implies that the mutations *per se* did not significantly perturb the structure at neutral or acidic pH.

Proximity Relationships. Proximity relationships between pairs of Cys residues have been studied in many proteins (Sen & Chakrabarti, 1990; Wang *et al.*, 1992), including the membrane protein, *E. coli* lactose permease (Jung *et al.*, 1993), by labeling their sulfhydryls with pyrene groups and monitoring excimer fluorescence. With the sulfhydryl-specific reagent, *N*-(1-pyrenyl)maleimide (PM), excimer fluorescence may be detected when the pyrene groups are within about 3.5 Å. The fluorescence emission spectrum of PM-labeled proteins (excited at 344 nm) shows two bands: a structured band, with peaks in the range of ~380–420 nm, from an excited pyrene monomer and an unstructured, broad band centered near 475 nm from the excited-state dimer (excimer).

Reduced forms of T domain (85 nM) containing the various Cys replacements were reacted with PM, and after the removal of unreacted reagent, the fluorescence emission spectra of the modified proteins were recorded. As shown in Figure 6A,B, typical pyrene excimer fluorescence (a broad peak centered around 475 nm) was observed with the double Cys mutants (C235/C351 and C291/C351) at both neutral pH (7.5) and low pH (5.0). The addition of liposomes (a final concentration of 33 μM phospholipid, so that the molar ratio of protein/phospholipid was 1:390) caused the virtual disappearance of the excimer in both mutant proteins at low pH. No change was seen with either protein upon liposome addition at pH 7.5, however, implying that at neutral pH both N235C and S291C are in close proximity to V351C in the presence or absence of liposomes. Thus, the proximity of both C235 and C291 to C351 was apparently maintained at low pH in the absence of liposomes, and their separation occurred only upon the addition of liposomes.

To confirm that the excimer fluorescence observed with the C235/C351 and C291/C351 proteins was the result of intramolecular, rather than intermolecular, interactions, we analyzed each of the corresponding PM-labeled single Cys mutants (C235, C291, and C351) at a protein concentration of 85 or 170 nM. At neutral pH and low pH, with or without liposomes, the emission spectra exhibited characteristic monomer fluorescence bands, and no excimer band at 475 nm was observed. Also, when pairs of single mutant proteins were mixed—C235 with C351 and C291 with C351—again, no excimer was observed (at either pH 5 or 7.5). Therefore, the excimer fluorescence observed with PM-labeled C235/

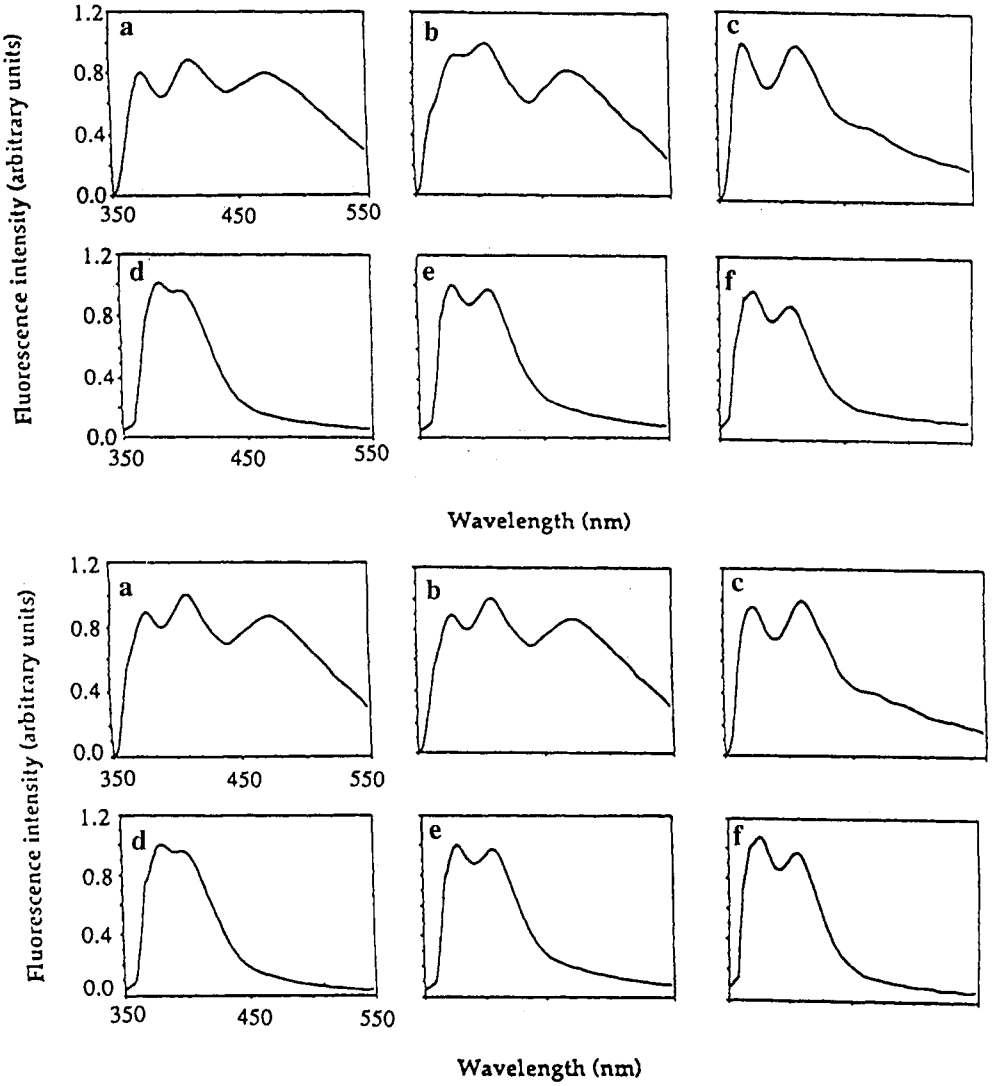

FIGURE 6: Fluorescence emission spectra of *N*-(1-pyrenyl)maleimide-labeled Cys mutant T domains. Top set of panels: (a) N235C/V351C, pH 7.5; (b) N235C/V351C, pH 5.0; (c) N235C/V351C, pH 5.0 + liposomes; (d) N235C, pH 7.5; (e) V351C, pH 7.5; (f) N235C + V351C, pH 7.5. Bottom set of panels: (a) S291C/V351C, pH 7.5; (b) S291C/V351C, pH 5.0; (c) S291C/V351C, pH 5.0 + liposomes; (d) S291C, pH 7.5; (e) V351C, pH 7.5; (f) S291C + V351C, pH 7.5. The final concentration of each protein was 85 nM, and the final phospholipid concentration was 33 μM. Spectra for N235C, V351C, or the mixture at low pH (5.0) in the presence or absence of liposomes were similar to those at pH 7.5 (data not shown). Similar results were obtained for S291C, V351C, and the mixture of both (data not shown). All spectra were obtained at 25 °C. The excitation wavelength was 344 nm.

C351 and C291/C351 T domains results from the intramolecular interactions between pyrene molecules attached to the Cys residues.

DISCUSSION

Diphtheria toxin represents an interesting example of a soluble, globular protein that is transformed into an integral membrane protein under certain physiological conditions—in this case, the mildly acidic pH encountered by the toxin within the endosomal compartment. This transformation appears to be a prerequisite for the translocation of the toxin's catalytic domain from the endosomal compartment to the cytosol, a process that is common to many toxins that enzymically modify intracellular targets (Montecucco *et al.*, 1991). Elucidation of the membrane insertion and traversal processes of DT may yield a better understanding of this general aspect of toxin action and, additionally, insights into other normal and pathologic processes involving protein insertion into membranes.

Studies by Boquet, Pappenheimer, and their co-workers (Boquet & Pappenheimer, 1976; Boquet *et al.*, 1976) first implicated the amino-terminal region of diphtheria toxin's B fragment as being hydrophobic and able to insert into detergent micelles. After acidic conditions were identified as the trigger for membrane translocation (Sandvig & Olsnes, 1980; Draper & Simon, 1980), the toxin and certain fragments of it (including B_{45}, a fragment corresponding approximately to the T domain) were found to produce ion-conductive channels in membranes under the influence of acidic pH (Kagan *et al.*, 1981; Donovan *et al.*, 1981). The availability of the crystallographic model of the soluble toxin now makes the description of its integral membrane form and the mechanism of insertion a more feasible goal. Recently, various lines of study have focused attention on a buried apolar structural element within the T domain, the TH8–TH9 helical hairpin, as an insertion motif that may become exposed and penetrate into the membrane under acidic conditions. This model is consistent with the finding that the TH8–TH9 peptide is protected from pronase digestion after membrane insertion of DT (Cabiaux *et al.*, 1994). The results presented here provide support for the TH8–TH9 insertion model and yield insight into the unfolding and membrane insertion processes.

We have studied the conformation of the isolated T domain under various conditions, taking advantage of the fact that the domain *per se* contains no native Cys residues and thus provides an ideal background for employing Cys substitutions and sulfhydryl chemistry. The formation of a disulfide bridge linking the TH8–TH9 and TH5–TH7 hairpins (C291/C351), which constrained the movement of the two hairpins relative to one another, markedly reduced the accessibility of apolar surfaces of the T domain to the hydrophobic fluorophore, TNS, as the pH was titrated below pH 5.5. Similar results were obtained with the C235/C351 mutant, in which the loop region of TH8–TH9 is linked to that of TH1–TH4, despite a higher background due to less efficient disulfide formation. Both of these artificial disulfides also strongly inhibited channel formation by the T domain in artificial bilayers. Control experiments showed that the reduced forms of the Cys double mutants were unaffected in unfolding and membrane insertion.

These results imply that each of these artificial disulfides prevents the T domain from adopting a conformation required for membrane insertion and channel formation. Single-channel conductance studies of other mutant forms of DT have strongly suggested that the TH8–TH9 hairpin spans the bilayer after insertion and that its helical hairpin motif in the native protein is largely preserved in the membrane. Because of its polar character, the TH1–TH4 layer seems unlikely to ever undergo insertion, and there currently is no evidence to support the earlier proposal that the TH5–TH7 hairpin also inserts. Thus, the TH8–TH9 hairpin seems likely to span the bilayer without the association (at least within the hydrocarbon core) of any other structural element of the T domain. If this is the case, then disulfide tethering of the TH8–TH9 hairpin of the T domain to either of its two contiguous helical layers would be expected to obstruct contact of the apolar surfaces of helices TH8 and TH9 with the hydrocarbon core of the membrane, thereby blocking stable integration and channel formation.

To complement the results obtained with the disulfide-trapping approach, we used the same double Cys mutants to probe the pathway of unfolding followed by the T domain before and during insertion. The reduced form of each of the double mutants was reacted with a pyrene fluorophore, which permitted monitoring of the proximity of the Cys-containing loops under various conditions. A strong excimer band was seen with the pyrene derivatives of both the C291/C351 and C235/C351 mutants at pH 7.5, which is consistent with the close proximity of these sites in the crystallographic structure of whole DT. Appropriate controls with the single Cys mutants confirmed that the excimer fluorescence was in fact due to intramolecular interactions of the fluorophores. When the pH was reduced to 5.0, the intensity of excimer fluorescence remained undiminished with both mutants, indicating that the T domain remained in a compact, folded form in solution at acidic pH. The addition of phospholipid vesicles to either of the double Cys mutants at pH 5.0 caused a marked reduction in the intensity of the excimer band, reflecting movement of adjacent protein layers away from the TH8–TH9 hairpin upon its interaction with the bilayer.

A variety of reports have documented the fact that low pH serves as a trigger for an unfolding step that exposes buried apolar surfaces in diphtheria toxin, but the extent of unfolding in aqueous solution has remained uncertain. The PM excimer studies suggest that no drastic movements of the three helical layers relative to one another occur in solution at pH 5.0 and that the T domain remains compact and monomeric, at least when the protein concentration is kept low, to minimize protein: protein collisions. The inherent assumption that the free energy of binding of the pyrene rings plays a very small role in maintaining folding at acidic pH in this experiment is supported by other data from electron paramagnetic studies with the T domain, including measurements of spin:spin coupling of the same double Cys mutants labeled with spin probes (Oh *et al.*, unpublished result). Circular dichroism and Fourier transform infrared measurements indicate that secondary structure is largely retained at acidic pH (Cabiaux *et al.*, 1989). The protein apparently adopts a molten globule state under acidic conditions, in which tertiary structure becomes fluid, while secondary structure remains intact. Transient exposure of its apolar surfaces through enhanced "breathing" of the structure at low pH apparently permits the T domain to bind to apolar entities with which it comes into contact, such as detergents, hydrophobic probes, or lipid vesicles. The results presented here suggest that the concept that binding of hydrophobic probes, such as TNS, implies that unfolding may not be correct. The apparent discrepancy between the results with pyrene-labeled T domain, implying the retention of tertiary structure at low pH, and the findings with TNS, suggesting unfolding under similar conditions, may be resolved by assuming that the fluorophore intercalates between hydrophobic surfaces within the protein that have become more mobile relative to one another at low pH, rather than binding to hydrophobic surfaces that have become exposed to solvent.[4] A more detailed study of the structure of complexes between hydrophobic probes, such as TNS, and proteins may resolve this paradox.

These data permit one to propose a more refined model of the process of unfolding and membrane insertion by the T domain within DT. After endocytosis, receptor-bound toxin is exposed to progressively lower pH values within the endosomal compartment. Acidic conditions may well have more than one effect on folding, perhaps including the weakening of electrostatic interactions between the domains, as suggested by Bennett *et al.* (1993), as well as within domains. Regardless, it is clear that a conformational change in the toxin's T domain at acidic pH is crucial to the process of membrane insertion. As shown here, conformational constraints imposed by a disulfide bridge between the TH8–TH9 hairpin and either of the other helical layers inhibits partial unfolding in solution and channel formation in membranes, and we infer that membrane insertion of the holotoxin would be blocked by these constraints. The results obtained with PM-labeled T domain suggest that, in the absence of membranes, the T domain of the toxin would remain in molten globule form (neglecting possible perturbing forces exerted by interactions and conformational alterations of the attached catalytic and receptor-binding domains). The results of liposome interaction with the pyrene-labeled double Cys mutants suggest that membrane contact is an essential component of the triggering mechanism that induces partial unfolding as a prelude to insertion of the TH8–TH9 hairpin.

How membrane contact may trigger unfolding remains uncertain, but electrostatic interactions between the phospholipid head groups of the membrane with positively charged regions of the T domain could be the crucial factor. As noted by Choe *et al.* (1992), the T domain shows a marked asymmetry in polar residues (and hydrophobicity), with 15 of its 16 Arg and Lys residues and all 6 of its His residues located on the side opposite the sites where we introduced Cys

[4] Our finding that varying the concentration of TNS has virtually no effect on the pH dependence profile of fluorescence (see Results) suggests that TNS does not induce protein unfolding under these conditions.

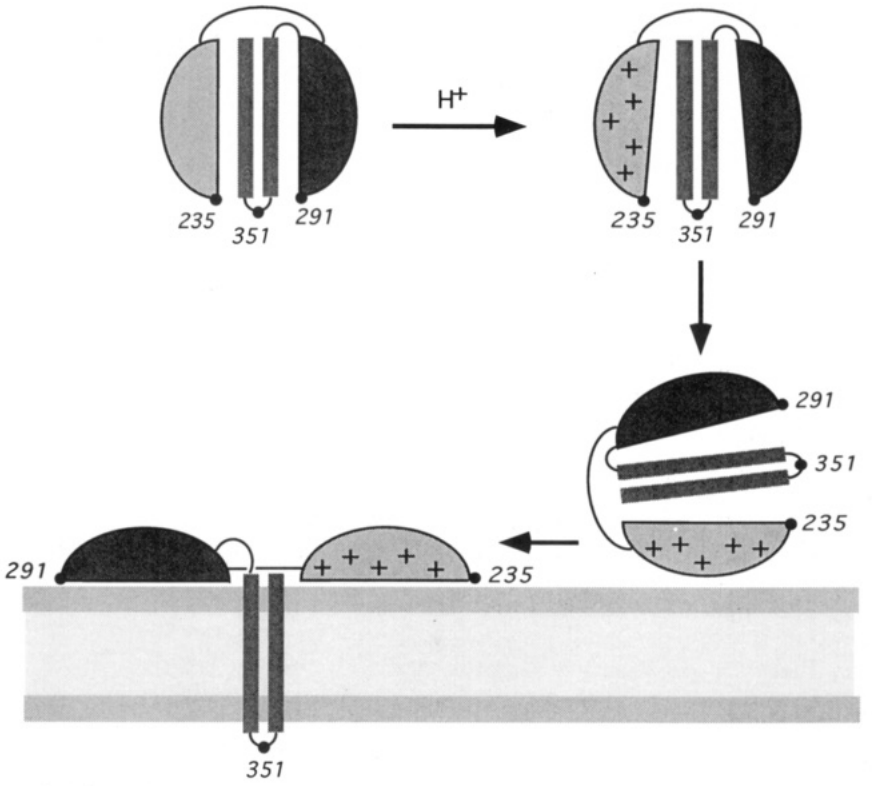

FIGURE 7: **7**: Schematic model of steps in the pH-dependent insertion of the T domain into a lipid bilayer. In the native T domain (upper left), the following are represented: the outermost layer (TH1–TH4, light shading), containing Asn235; the intermediate layer (TH5–TH7, intermediate shading), containing Ser291; and the TH8–TH9 helical hairpin (dark shading), containing Val351 at its tip. The steps in membrane insertion shown are as follows: first, protonation at acidic pH, resulting in a state in which the secondary structure is largely retained, together with fluid tertiary structure; second, binding of this form to the membrane via the positively charged surface of the TH1–TH4 layer, which triggers separation of the TH1–TH4 and TH5–TH7 layers from the helical hairpin layer; and finally, insertion of the TH8–TH9 hairpin into the bilayer, such that the tip penetrates to the opposite face of the bilayer. The TH1–TH4 layer contains one Arg (210), ten Lys (212, 214, 216, 221, 227, 229, 236, 242, 244, 264), three His (223, 251, 257), three Asp (205, 207, 211), and ten Glu (218, 222, 232, 240, 241, 248, 249, 256, 259, 262), which would be expected to yield a net charge close to zero for this region at neutral pH and a strong positive charge at acidic pH's.

residues in the current study. Under acidic conditions this polar face of the molecule, which includes the TH1–TH4 helices and loop regions between the three helical layers, would be strongly positively charged and could serve as the initial site of contact with the negatively charged membrane. Electrostatic interactions with the bilayer could thus serve as the energy source for separation of the three layers within the molten globule structure, and this would, in turn, expose the apolar interfaces between them and permit contact of these surfaces with transiently exposed hydrocarbon chains of the bilayer core. Protonation of the two acidic residues at the tip of the TH8–TH9 hairpin (E349 and D352) under acidic conditions would reduce the energy barrier of insertion. Under such conditions, the TH8–TH9 hairpin would adopt a transmembrane configuration, and the acidic tip residues would be expected to reionize in the neutral pH of the cytosol, while the TH1–TH4 and perhaps TH5–TH7 helices would remain at the membrane surface within the endosomal lumen. The transition process is summarized in Figure 7.

The requirement of membrane insertion by the TH8–TH9 hairpin for the lethal action of DT is demonstrated by the inhibitory effect of a positively charged residue either at the TH8–TH9 dagger tip (Lys at position 349 or 352) (O'Keefe *et al.*, 1992; Silverman *et al.*, submitted for publication) or on the apolar face of TH9 (an I364K mutation) (Cabiaux *et al.*, 1993). Disulfide linking of the TH8–TH9 layer to either TH1–TH4 or TH5–TH7 presumably would have a similar inhibitory effect, but we were unable to test this hypothesis in whole DT, because of complications arising from reduction of the native disulfide linking the catalytic domain (fragment A) to the T and R domains (fragment B).

While information about the mechanisms of membrane insertion and translocation by DT is accumulating at an accelerating pace, our overall knowledge of these processes remains limited. Additional data are needed concerning the locations, conformations, and interactions of the three layers of the T domain, and of the three domains of the toxin, during toxin insertion and translocation. Various models have been proposed concerning the pathway by which the catalytic A fragment crosses the membrane, including penetration via the aqueous channel formed by the T domain, but the actual mechanism remains unknown (London, 1992). The approach illustrated by the present work, in which the power of directed mutagenesis is combined with biophysical and biochemical tools, can be expected to yield further insights into such mechanisms.

Three-layer, α-helical structures have also been found within other bacterial protein toxins such as colicin A and δ-endotoxin of *Bacillus thuringiensis* (Parker *et al.*, 1989; Li *et al.*, 1991). The basic fold consists of a bundle of between 7 and 10 α-helices organized in three layers, which represents a soluble form of packaging for the apolar and amphipathic helices that are used to insert into the membrane (Parker & Pattus, 1993). The mechanism of unfolding and insertion proposed for the T domain of DT resembles the "umbrella" conformation of colicin A, as originally proposed by Parker and co-workers (1992). Recent studies of colicin A involving fluorescence energy measurements (Lakey *et al.*, 1993) and disulfide bond

engineering (Duché *et al.*, 1994) favor a different model, however, in which the buried apolar hairpin does not insert perpendicular to the plane of the membrane, but rather, lies parallel to the membrane surface. The tip of this hairpin, however, is devoid of polar residues corresponding to the acidic residues found at the tip of the TH8–TH9 hairpin of DT, which may account for the apparently different orientation after insertion. Further studies of such proteins may reveal features that will shed light on normal, as well as pathogenic, processes involving protein insertion and penetration of membranes.

REFERENCES

Ausubel, F., Brent, R., Kingston, R., Moore, D., Seidman, J., Smith, J., & Struhl, K., Eds. (1987) *Current Protocols in Molecular Biology*, Greene-Wiley Interscience, New York.

Bennett, M. J. (1993) Dissertation, University of California, Los Angeles, CA.

Blewitt, M. G., Chung, L. A., & London, E. (1985) *Biochemistry 24*, 5458–5464.

Boquet, P., & Pappenheimer, A. M., Jr. (1976) *J. Biol. Chem. 251*, 5770–5778.

Boquet, P., Silverman, M. S., Pappenheimer, A. M., Jr., & Vernon, W. B. (1976) *Proc. Natl. Acad. Sci. U.S.A. 73*, 4449–4453.

Cabiaux, V., Brasseur, R., Wattiez, R., Falmagne, P., Ruysschaert, J. M., & Goormaghtigh, E. (1989) *J. Biol. Chem. 264*, 4928–4938.

Cabiaux, V., Mindell, J., & Collier, R. J. (1993) *Infect. Immun. 61*, 2200–2202.

Cabiaux, V., Quertenmont, P., Conrath, K., Brasseur, R., Capiau, C., & Ruysschaert, J. (1994) *Mol. Microbiol. 11*, 43–50.

Careaga, C. L., & Falke, J. J. (1992) *J. Mol. Biol. 226*, 1219–1235.

Choe, S., Bennett, M. J., Fujii, G., Curmi, P. M. G., Kantardjieff, K. A., Collier, R. J., & Eisenberg, D. (1992) *Nature 357*, 216–222.

Collier, R. J. (1990) *ADP-Ribosylating Toxins and G Proteins: Insights into Signal Transduction* (Moss, J., & Vaughan, M., Eds.) pp 3–19, American Society for Microbiology, Washington, D.C.

Collins, C. M., & Collier, R. J. (1987) *Membrane-Mediated Cytotoxicity* (Bonavida, B., & Collier, R. J., Eds.) pp 41–52, Alan R. Liss, Inc., New York.

Davis, B. D., Dulbecco, R., Eisen, H. N., & Ginsberg, H. S. (1990) *Microbiology*, 4th ed., J. B. Lippincott Company, Philadelphia.

DeLeers, M., Beugnier, N., Falmagne, P., Cabiaux, V., & Ruysshcaert, J. M. (1983) *FEBS Lett. 160*, 82–86.

Donovan, J. J., Simon, M. I., Draper, R. K., & Montal, M. (1981) *Proc. Natl. Acad. Sci. U.S.A. 78*, 172–176.

Draper, R. K., & Simon, M. I. (1980) *J. Cell Biol. 87*, 849–854.

Duche, D., Parker, M. W., Gonzalez-Manas, J., Pattus, F., & Baty, D. (1994) *J. Biol. Chem. 269*, 6332–6339.

Dumont, M. E., & Richards, F. M. (1988) *J. Biol. Chem. 263*, 2087–2097.

Dunten, R. L., Sahin-Toth, M., & Kaback, H. R. (1993) *Biochemstry 32*, 12644–12650.

Falke, J. J., & Koshland, D. E. (1987) *Science 237*, 1596–1600.

Greenfield, L., Bjorn, M. J., Horn, G., Fong, D., Buck, G. A., Collier, R. J., & Kaplan, D. A. (1983) *Proc. Natl. Acad. Sci. U.S.A. 80*, 6853–6857.

Hovde, C. J., Calderwood, S. B., Mekalanos, J. J., & Collier, R. J.. (1988) *Proc. Natl. Acad. Sci. U.S.A. 85*, 2568–2572.

Johnson, V. G., Nicholls, P. J., Habig, W. H., & Youle, R. J. (1993) *J. Biol. Chem. 268*, 3514–3519.

Jung, K., Jung, H., Wu, J., Prive, G. G., & Kaback, H. R. (1993) *Biochemistry 32*, 12273–12278.

Kabsch, W., & Sander, C. (1983) *Biopolymers 22*, 2577–2637.

Kagan, B. L., Finkelstein, A., & Colombini, M. (1981) *Proc. Natl. Acad. Sci. U.S.A. 78*, 4950–4954.

Kagawa, Y., & Racker, E. (1971) *J. Biol. Chem. 246*, 5477–5487.

Koehler, T., & Collier, R. J. (1991) *Mol. Microbiol. 5*, 1501–1506.

Kobashi, K. (1968) *Biochim. Biophys. Acta 158*, 139–145.

Kouyama, T., & Mihashi, K. (1981) *Eur. J. Biochem. 114*, 33.

Kyte, J., & Doolittle, R. F. (1982) *J. Mol. Biol. 157*, 105–132.

Laemmli, U. K. (1970) *Nature 227*, 680–685.

Lakey, J. H., Duche, D., Gonzalez-Manas, J., Baty, D., & Pattus, F. (1993) *J. Mol. Biol. 230*, 1055–1067.

Li, J. D., Carroll, J., & Ellar, D. J. (1991) *Nature 353*, 815–821.

London, E. (1992) *Biochim. Biophys. Acta 1113*, 25–51.

Mel, S. F., & Stroud, R. M. (1993) *Biochemistry 32*, 2082–2089.

Mindell, J. A., Silverman, J. A., Collier, R. J., & Finkelstein, A. (1994a) *J. Membr. Biol. 137*, 45–57.

Mindell, J. A., Zhan, H., Huynh, P. D., Collier, R. J., & Finkelstein, A. (1994b) *Proc. Natl. Acad. Sci. U.S.A. 91*, 5272–5176.

Montal, M. (1974) *Methods Enzymol. 32*, 545–554.

Montecucco, C., Papini, E., & Schiavo, G. (1991) in *Sourcebook of Bacterial Protein Toxins* (Alouf, J. E., & Freer, J. H., Eds.) pp 45–56, Harcourt Brace Jovanovich, Publishers, Sidcup, Kent, U.K.

Naglich, J. G., Metherall, J. E., Russell, D. W., & Eidels, L (1992) *Cell 69*, 1051–1061.

O'Keefe, D. O., & Collier, R. J. (1989) *Proc. Natl. Acad. Sci. U.S.A. 86*, 343–346.

O'Keefe, D. O., Cabiaux, V., Choe, S., Eisenberg, D., & Collier, R. J. (1992) *Proc. Natl. Acad. Sci. U.S.A. 89*, 6202–6206.

Pabo, C. O., & Suchanek, E. G. (1986) *Biochemistry 25*, 5987–5991.

Parker, M. W., & Pattus, F. (1993) *Trends Biochem. Sci. 18*, 391–395.

Parker, M. W., Pattus, F., Tucker, A. D., & Tsernoglou, D. (1989) *Nature 337*, 93–96.

Parker, M. W., Postma, J. P. M., Pattus, F., Tucker, A. D., & Tsernoglou, D. (1992) *J. Mol. Biol. 224*, 639–657.

Ptitsyn, O. B. (1987) *J. Protein Chem. 6*, 273–293.

Sandvig, K., & Olsnes, S. (1980) *J. Cell Biol. 87*, 828–832.

Sandvig, K., & Olsnes, S. (1981) *J. Biol. Chem. 256*, 9068–9076.

Sen, A. C., & Chakrabarti, B. (1990) *J. Biol. Chem. 265*, 14277–14284.

Silverman, J. A., Mindell, J. A., Zhan, H., Finkelstein, A., & Collier, R. J. (1994) *J. Membr. Biol. 137*, 17–28.

Studier, F. W., & Moffatt, B. A. (1986) *J. Mol. Biol. 189*, 113–130.

Wang, Z., Gergely, J., & Tao, T. (1992) *Proc. Natl. Acad. Sci. U.S.A. 89*, 11814–11817.

Wonderlin, W. F., Finkel, A., & French, R. J. (1990) *Biophys. J. 58*, 289–297.